3218–3227 *Nucleic Acids Research, 1997, Vol. 25, No. 16* *© 1997 Oxford University Press*

A two unit antisense RNA cassette test system for silencing of target genes

Hilde M. Engdahl*, Tord Å. H. Hjalt[1] and E. Gerhart H. Wagner

Department of Microbiology, Swedish University of Agricultural Sciences, Genetic Center, Box 7025, Genetikvägen 1, S-75007 Uppsala, Sweden and [1]Department of Microbiology, Uppsala University, Biomedical Center, Box 581, S-75123 Uppsala, Sweden

Received May 19, 1997; Revised and Accepted June 26, 1997

ABSTRACT

This communication describes a two unit antisense RNA cassette system for use in gene silencing. Cassettes consist of a recognition unit and an inhibitory unit which are transcribed into a single RNA that carries sequences of non-contiguous complementarity to the chosen target RNA. The *recognition* unit is designed as a stem–loop for rapid formation of long-lived binding intermediates with target sequences and resembles the major stem–loop of a naturally occurring antisense RNA, CopA. The *inhibitory* unit consists of either a sequence complementary to a ribosome binding site or of a hairpin ribozyme targeted at a site within the chosen mRNA. The contributions of the individual units to inhibition was assessed using the *lacI* gene as a target. All possible combinations of recognition and inhibitory units were tested in either orientation. In general, inhibition of *lacI* expression was relatively low. Fifty per cent inhibition was obtained with the most effective of the constructs, carrying the recognition stem–loop in the antisense orientation and the inhibitory unit with an anti-RBS sequence. Several experiments were performed to assess activities of the RNAs *in vitro* and *in vivo*: antisense RNA binding assays, cleavage assays, secondary structure analysis as well as Northern blotting and primer extension analysis of antisense and target RNAs. The problems associated with this antisense RNA approach as well as its potential are discussed with respect to possible optimization strategies.

INTRODUCTION

Antisense strategies for gene silencing have attracted much attention in recent years (1,2). The underlying concept is simple yet (in principle) effective: antisense nucleic acids (NA) base pair with a target RNA resulting in inactivation. Target RNA recognition by antisense RNA or DNA can be considered a hybridization reaction, although this view is sometimes clearly misleading (see below). Since the target is bound through sequence complementarity, this implies that an appropriate choice of antisense NA should ensure high specificity. Inactivation of the targeted RNA can occur via different pathways, dependent on the nature of the antisense NA (either modified or unmodified DNA or RNA) and on the properties of the biological system in which inhibition is to occur, i.e. the sum of the metabolic activities that mediate inhibition.

Major differences between exogenous [antisense oligo(deoxy)-ribonucleotides; AONs] and endogenous antisense RNA strategies lie in: (i) delivery of the inhibitor; (ii) presumed mode of binding to the target RNA; (iii) details of the inhibitory reaction. AONs are generally applied extracellularly and taken up, whereas antisense RNAs are most often transcribed intracellularly, after transient or stable introduction of an appropriate antisense gene (1,3). AONs are designed to contain a low degree of secondary structure in order to permit efficient hybridization, whereas antisense RNAs are often larger and structurally more complex. The latter implies that binding reactions, unlike the AON case, occur between *folded* RNAs and therefore may follow different rules. Antisense DNA approaches often rely on endogenous RNase H activity to inactivate the target RNA. Numerous modifications of AONs have been introduced, resulting in metabolically more stable compounds and those with altered stereochemistry (see for example 4). In contrast, antisense RNA-mediated silencing can occur by duplex-dependent blockage of a ribosome binding site (RBS) within an mRNA, duplex-dependent facilitated mRNA decay, antisense RNA-induced premature termination of transcription and cleavage of the mRNA by an antisense RNA with ribozyme activity. Inhibition of gene expression by introduced antisense RNA genes has been achieved in, for example, bacteria (5), plants (6) and mammalian cells (7).

Numerous naturally occurring antisense RNA systems have been found in bacterial accessory DNA elements, such as phages, plasmids and transposons (for a review see 8). These systems are useful sources of information regarding binding rate, specificity and mechanisms of target RNA inactivation. The copy number control circuit of bacterial plasmid R1 with its key elements CopA (antisense RNA) and CopT (target) has been studied extensively. Its efficiency, both in terms of binding rate and specificity (9–12), prompted us to design antisense RNA cassettes that incorporate favourable characteristics of this system. In particular, it is known that stem–loop II (SL II) of CopA suffices for ‘kissing complex’ formation with the target RNA and that formation of this transient, but long-lived, intermediate is rate limiting for pairing (11).

The basic features of the cassette are as follows: a promoter is located upstream of a sequence which is either complementary to a chosen RBS or encodes a ribozyme targeted against a sequence within the mRNA; downstream of this region a stem–loop is encoded, designed to serve as a CopA-like recognition structure

* To whom correspondence should be addressed. Tel: +46 18 673380; Fax: +46 18 673392; Email: engdahl@mikrob.slu.se

Downloaded from https://academic.oup.com/nar/article/25/16/3218/1454766 by guest on 10 April 2024

and a transcription terminator. The (extended) loop sequence is complementary to a short segment within the target RNA. Thus, the RNA contains two non-contiguous regions of complementarity; one (the stem–loop) represents the *recognition unit*, which promotes rapid and transiently stable binding (but not complete duplex formation), whereas the second is the *inhibitory unit* (anti-RBS or hairpin ribozyme). The overall rate of interaction with and inactivation of the target RNA is expected to be determined by the stem–loop (rapid formation of a 'kissing complex'; see above). After this concentration-dependent initial step, subsequent base pairing of the inhibitor unit to its target segment will occur in principle *intra*molecularly, i.e. independent of concentration and, hence, should not be rate limiting.

We describe here a set of antisense RNA and (as controls) sense RNA constructs aimed at a model target in *Escherichia coli*, the *lacI* mRNA (13). Inhibition was measured as inhibition of LacI–LacZ fusion protein synthesis *in vivo* and the structural and inhibitory properties of the various RNAs were assessed *in vitro*.

MATERIALS AND METHODS

Bacterial strains and plasmids

The *Escherichia coli* strain DH5α (F⁻ *endA1*, *hsdR17*, *supE44*, *thi-1*, *recA1*, *gyrA96*, *relA1*, Δ[*argF-lacZYA*]*U169*, *Φ80ΔlacZ-ΔM15*; 14) was used for plasmid construction. Strain XAc (F′ Δ14[*pro lac*] *ara*, *gyrA*, *rpoB*, *argE* (UAG); 15) was used for measurements of LacI–LacZ fusion protein synthesis.

Plasmids used are listed in Table 1. Plasmid pGW47 is a ColE1 vector that contains the complete *copA* gene of plasmid R1, inserted into the *Bam*HI site of pMc5-8 (16; *Bam*HI site destroyed). To create plasmid pGW47-1 two polymerase chain reactions (PCRs) were performed using primers HE3/HE5 and HE4/HE6 respectively on pGW47 DNA. The two PCR fragments were cleaved with *Eco*RI and *Bam*HI (pair 3/5) and *Bam*HI and *Xba*I (pair 4/6) respectively and ligated to plasmid DNA of pGW47, cleaved with *Eco*RI and *Xba*I. The resulting plasmid, pGW47-1, lacks the *Sma*I site of pGW47, has acquired a *Bam*HI–*Hin*dIII sequence between the *copA* promoter and the 5′-end of SL II and carries an *Xba*I site just downstream of the SL II terminator. Subsequently we replaced the wild-type sequence of SL II by a double-stranded DNA fragment encoding a *copA* SL II sequence containing two *Sma*I/*Xma*I sequences (Fig. 2), resulting in pGW48. The DNA segment between the two *Sma*I sites was replaced by a double-stranded DNA fragment (HE12/HE13) containing a *lacI* sequence, to yield pGW48-a and pGW48-s respectively (Figs 1 and 2). Plasmids pGW48-a and pGW48-s were the parents of all subsequent constructs: double-stranded DNA fragments (see below) were inserted into the unique *Hin*dIII site to place anti-RBS or ribozyme sequences, in either orientation, between the promoter and the stem–loop.

Cell growth and media

Cells were grown in LB medium (17) supplemented with 0.2% glucose. LA solid medium was LB medium with 1.5% (w/v) agar. When appropriate, chloramphenicol (30 μg/ml) was included. M9 medium (18) was used as minimal medium. Solid medium contained 10 g Sicomol agar/l and was supplemented with 0.2% glucose, chloramphenicol (30 μg/ml), arginine (70 μg/ml), proline (46 μg/ml) and thiamine (1 μg/ml). X-Gal (5-bromo-4-chloro-3-indolyl-β-galactopyranoside) was used at a final concentration of 40 μg/ml.

Enzymes and chemicals

Restriction enzymes for cloning procedures were bought from Amersham, New England Biolabs or Pharmacia. Radiochemicals were purchased from Amersham or DuPont NEN.

Table 1. Plasmids used

Plasmids[a]	Description	Parent plasmid(s)	Source/reference
pMc5-8	pBR325-derived cloning vector		16
pGW47	*copA* gene of plasmid R1 (*Sau*3A fragment) cloned in ColE1-vector	pMc5-8 + pKN505	This work
pGW47-1	Removed unique *Sma*I site in vector, introduced unique *Bam*HI and *Hin*dIII sites	pGW47	This work
pGW48	SL II sequence with flanking *Sma*I sites	pGW47-1	This work
pGW48-a	SL II with antisense *lacI* sequence inserted	pGW48	This work
pGW48-s	SL II with sense *lacI* sequence inserted	pGW48	This work
pGW48-a-rbs	Contains antisense *lacI* RBS sequence	pGW48-a	This work
pGW48-a-sbr	Contains sense *lacI* RBS sequence	pGW48-a	This work
pGW48-a-rib	Contains antisense *lacI* ribozyme sequence	pGW48-a	This work
pGW48-a-bir	Contains inverted ribozyme sequence	pGW48-a	This work
pGW48-s-rbs	Contains antisense *lacI* RBS sequence	pGW48-s	This work
pGW48-s-sbr	Contains sense *lacI* RBS sequence	pGW48-s	This work
pGW48-s-rib	Contains antisense *lacI* ribozyme sequence	pGW48-s	This work
pGW48-s-bir	Contains inverted ribozyme sequence	pGW48-s	This work

[a]Constructions are described in Materials and Methods.

Downloaded from https://academic.oup.com/nar/article/25/16/3218/1454766 by guest on 10 April 2024

DNA manipulations

Purification of plasmid DNA, restriction enzyme cleavages and other DNA techniques were essentially according to Sambrook *et al*. (19).

Oligodeoxyribonucleotides

Oligodeoxyribonucleotides were synthesized on an Applied Biosystems 394 DNA/RNA Synthesizer or bought from Pharmacia (Sweden). Sequencing primers for all plasmid inserts were HE7 (5′-GTG ATC TTC CGT CAC A) or HE8 (5′-AGG AGC CTT TAA TTG TAT). For construction of pGW47, two pairs of PCR primers were used, HE3 (5′-ATA TGA ATT CCT CGG GAT CAG TCA C) and HE5 (5′-ATA TGG ATC CTG CGG GGA GTA TAG TTA TAT) and HE6 (5′-ATA TGG ATC CAA GCT TGG GCC CCG GTA ATC TTT T) and HE4 (5′-TAT ATC TAG AGG CAA GGA ACT GGT TCT GAT). For insertion of the *copA* SL II sequence containing two *Sma*I sites we used HE12 (5′-AGC TTG GGC CCG GGT AAT CTT TTC GTA CTC GCC AAA GTT GAA GAA GAT TAC CCG GGT TTT TGC TTT T) and HE 13 (5′-CTA GAA AAG CAA AAA CCC GGG TAA TCT TCT TCA ACT TTG GCG AGT ACG AAA AGA TTA CCC GGG CCC A). To introduce *lacI* sequences into the SL II loop of pGW48 we used the pair HE18 (5′-CCG GGT AAT CTT TTC TGA CTC TCT TCA GTT GAA GAA GAT TAC) and HE19 (5′-CCG GGT AAT CTT CTT CAA CTG AAG AGA GTC AGA AAA GAT TAC). For insertion of *lacI* rbs/sbr sequences into pGW48-a/pGW48-s the pair HE16 (5′-AGC TTA GGG TGG TGA ATG TGA AAC CAG TAA CGT TAT ACG ATG TA) and HE17 (5′-AGC TTA CAT CGT ATA ACG TTA CTG GTT TCA CAT TCA CCA CCC TA) were used. HE14 (5′-AGC TTG AAA CGA GAA GAT AAC CAG AGA AAC ACA CGT TGT GGT ATA TTA CCT GGT A) and HE15 (5′-AGC TTA CCA GGT AAT ATA CCA CAA CGT GTG TTT CTC TGG TTA TCT TCT CGT TTC A) served to introduce the ribozyme/inverted ribozyme sequence. As probes for Northern analyses, we used HE20 (5′-AAG ATT ACC CGG GCC CAA GCT T) and the 5S rRNA-specific oligo GW-5S (5′-TAC GGC GTT TCA CTT CTG AGT TTG GG). DNA templates for *in vitro* synthesis of antisense RNAs containing rbs/sbr and a- and s-SL II sequences by *E.coli* RNA polymerase were generated by PCR from appropriate plasmid DNA templates with primers HE27 (5′-GTG ATC TTC CGT CAC AGG TAT) and HE25 (5′-GGT GAA TTT CGA CCT CTA GA). Primers for synthesis of *lacI* mRNA transcription templates were HE21 (5′-GAA ATT AAT ACG ACT CAC TAT AGG AAG AGA GTC AAT TCA G) and HE22 (5′-CCG CTT CCA CTT TTT C). PCR primers for generating transcription templates containing rib and a-/s-SL II were HE23 (5′-GAA ATT AAT ACG ACT CAC TAT AGG ATC CAA GCT TGA AAC) and HE25. For the bir templates, containing the inverted sequences, primers HE24 (5′- GAA ATT AAT ACG ACT CAC TAT AGG ATC CAA GCT TAC CAG) and HE25 were used. HE21, HE23 and HE24 contain T7 RNA polymerase promoter sequences. Primer extension on ribozyme-cleaved *lacI* mRNA was done with HE22, as was *in vivo* 5′-end mapping of *lacI* mRNA.

Synthesis of PCR fragments for use as *in vitro* transcription templates

We used suitable pairs of primers (see above) to synthesize all *in vitro* transcription templates. PCR to obtain templates for T7 RNA polymerase transcription of *lacI* RNA (149 nt) and ribozyme-containing RNAs (148 nt) was performed as described (20). The same protocol was used to obtain DNA templates of rbs-/sbr-containing RNAs (296 nt). These fragments contain the *copA* promoter. PCR products were eluted from gels with DEAE–cellulose membranes (KEBO) according to Dretzen *et al*. (21). DNA fragments were dissolved in 30 µl TE buffer (10 mM Tris–HCl, pH 7.9, 1 mM Na_2EDTA).

In vitro transcription of RNAs

For secondary structure analysis of 5′-end-labelled SL II RNAs (Fig. 3), supercoiled plasmid DNA of the pGW47/48 series was transcribed by *E.coli* RNA polymerase (Pharmacia) with [γ-^{32}P]ATP and unlabelled NTPs as in Persson *et al*. (9). The RNAs used for binding studies (Fig. 5) were transcribed from linear, PCR-generated templates according to the same protocol, but including [α-^{32}P]UTP and unlabelled NTPs. Ribozyme sequence-containing RNAs were transcribed by T7 RNA polymerase from PCR-generated DNA templates as described (9,20). [^{3}H]UTP was included to permit quantification of the amounts purified. Transcription of *lacI* RNA was with [α-^{32}P]UTP (Fig. 6A) or [^{3}H]UTP (Figs 5 and 6B).

Secondary structure probing of SL II RNAs with RNases A, T1 and T2

Structural mapping of 5′-end-labelled RNAs was performed as described previously (20,22,23).

Northern blot analysis

Isolation of total cellular RNA and Northern analysis were as described (23,24). As a probe, an end-labelled oligodeoxyribonucleotide complementary to a sequence present in all RNAs investigated (HE20) was used. Reprobing for 5S rRNA was done as described (23). Band intensities were quantified using a Molecular Dynamics PhosphorImager.

In vitro binding assays

Binding of uniformly ^{32}P-labelled antisense RNAs to unlabelled *lacI* target RNAs was assayed by gel shift analysis and calculations of the apparent second order binding rate constants (k_{app}) performed as described previously (9,11). In all cases, a high (>10-fold molar) excess of target RNA (concentration 1.3×10^{-8} M) over labelled antisense RNA was used to ensure pseudo-first order kinetics.

In vitro ribozyme assay

In vitro cleavage experiments with hairpin RNA constructs were performed according to Chowrira and Burke (25). Reactions contained 20 pmol ^{3}H-labelled ribozyme and 0.5 pmol ^{32}P-labelled *lacI* RNA in standard reaction buffer (40 mM Tris–HCl, pH 7.5, 12 mM $MgCl_2$, 2 mM spermidine) at 37°C. Aliquots were withdrawn at different time points and quenched by adding 4 µl ice-cold formamide dye. Samples were boiled for 1 min and electrophoresed on 8% sequencing gels, followed by autoradiography. For determination of the cleavage sites (Fig. 6B), reactions were done as above except that *lacI* RNA was unlabelled.

Downloaded from https://academic.oup.com/nar/article/25/16/3218/1454766 by guest on 10 April 2024

Primer extension analysis

Primer extensions (Fig. 7) were performed on ~10 µg total cellular RNA. Samples were boiled for 1 min in the presence of ^{32}P-end-labelled primer HE22 (~100 000 c.p.m.) in hybridization buffer (50 mM Tris–HCl, pH 7.9, 50 mM KCl). Mixtures were snap frozen in liquid nitrogen and subsequently thawed on ice. Incubation was at 45°C for 60 min in extension buffer (50 mM Tris–HCl, pH 7.9, 10 mM $MgCl_2$, 50 mM KCl, 10 mM DTT) containing 0.2 mM dNTPs, 13 U human placental ribonuclease inhibitor and 3.5 U AMV reverse transcriptase (both Amersham). After ethanol precipitation, samples were dissolved in water. An equal volume of formamide dye was added and samples boiled prior to loading (8% sequencing gel). Sequencing ladders were obtained on *lacI* DNA using a Thermal Cycle Sequencing kit (New England Biolabs). Primer extension on ribozyme-cleaved *lacI* RNA (Fig. 6B) was also performed with primer HE22.

In vivo lacI–lacZ expression assays

LacI–LacZ fusion protein synthesis was measured in cell extracts from exponentially growing cultures. The protocol was essentially as in Berzal-Herránz *et al*. (26), except that cultures were grown in M9 minimal medium supplied with 0.2% glucose.

RESULTS

Construction of plasmids encoding two unit antisense RNA cassette genes

We intended to test the feasibility of combining the properties of rapid target RNA binding and effective inhibition of target RNA function within a non-contiguous stretch of RNA encoded by a cassette gene. In order to assess the contributions of the two units, recognition and inhibitor (Fig. 1A), to overall inhibition, plasmids were constructed that encoded all units in either the sense or antisense orientation. The plasmid derivatives of the pGW48-a series all encode a recognition unit that carries 11 consecutive nucleotides complementary to the 5′-end region of the chosen target, *lacI* mRNA (Fig. 2). They also carry sequences either complementary to 38 nt encompassing the *lacI* RBS or a 55 nt ribozyme segment with two short flanking sequences of complementarity to a sequence of *lacI* mRNA located ~80 nt from its 5′-end (Fig. 2). The *lacI* RBS region targeted is predicted to contain a low degree of secondary structure (data not shown). The ribozyme unit was designed to conform to the extensively investigated hairpin ribozyme (27–30). In addition, inverted gene segments were introduced, to serve as ‘sense’ controls for both anti-RBS (rbs) and ribozyme (rib). These were denoted sbr and bir respectively (see schematics in Fig. 1B for RNAs encoded). Parallel series with predicted inactive recognition units (sense orientation) were derived in the same way from pGW48-s. For simplicity, we will in the following refer to all the encoded RNAs collectively as antisense RNA, disregarding the relative orientations of the two units.

Based on earlier experiments (data not shown), we anticipated that a certain number of controls would be required for adequate assessment of inhibitory activity dependent on the presence or absence of one or the other unit.

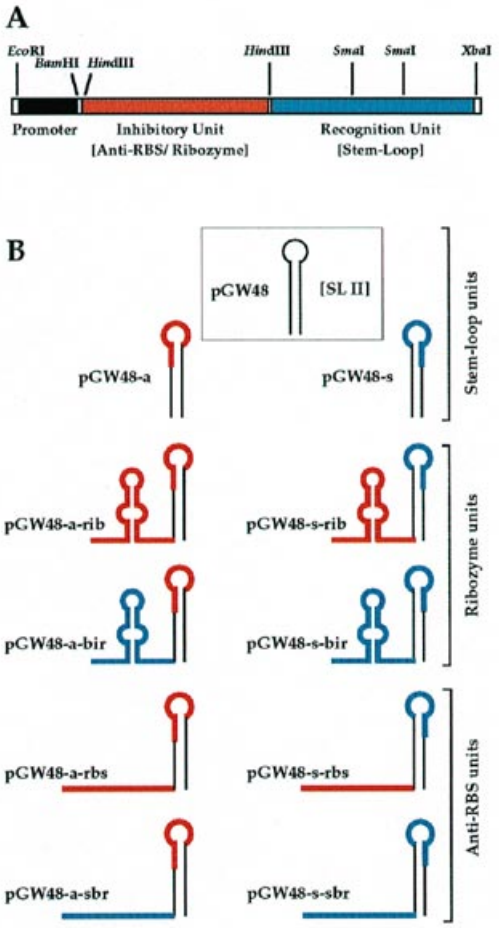

Figure 1. Schematic representation of the antisense gene cassette and RNAs encoded by plasmids of the pGW48 series. (**A**) The basic two unit antisense RNA cassette is shown. The positions of the promoter sequence, inhibitory unit and recognition unit respectively and relevant restriction sites are indicated. (**B**) RNAs encoded by plasmids of the pGW48 series (Materials and Methods) are shown schematically. Sequences complementary to the *lacI* target RNA are indicated in red and sequences in sense orientation are blue. For simplicity, the entire ribozyme sequence is shown coloured, even though only the flanking sequences are complementary to the target (see Fig. 2).

Secondary structures of the recognition unit segment of the antisense RNAs

Since the basic concept of the recognition unit was derived from previous studies of structural features that contribute to the binding rate of CopA (9–11,20,31), we compared the secondary structures of SL II (stem–loop II of CopA) to stem–loops containing *lacI* sequences in the antisense or sense orientation respectively (a-SL II and s-SL II; Fig. 2). Structure-specific RNases were used to map single-stranded regions of *in vitro* transcribed, 5′-end-labelled RNAs. Figure 3 (upper panel) shows autoradiograms of partial cleavage patterns obtained with RNase A (cleavage 3′ of single-stranded pyrimidines), T1 (single-stranded G residues) and T2 (single-stranded nucleotides with some preference for adenosines) and a schematic representation of the results (lower panel). All three stem–loops show indications of similar

Downloaded from https://academic.oup.com/nar/article/25/16/3218/1454766 by guest on 10 April 2024

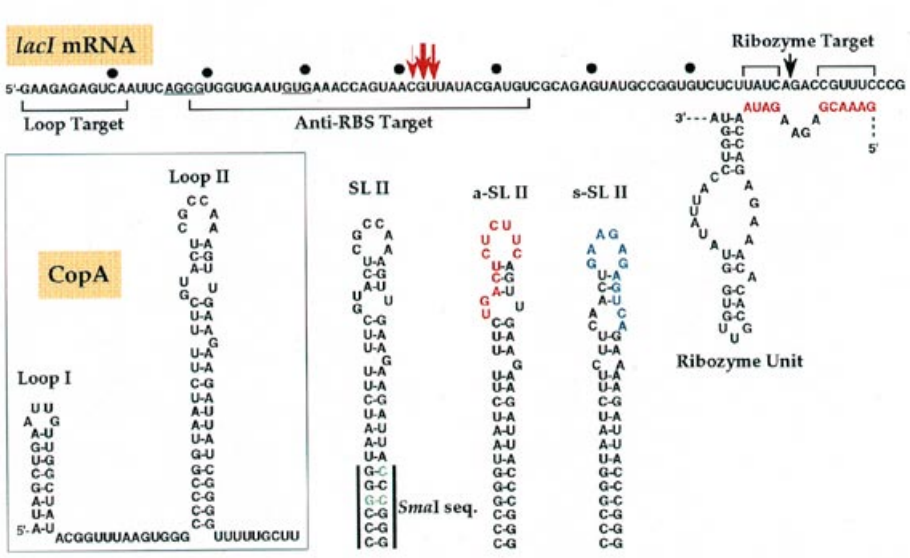

Figure 2. Relevant sequences and structures of antisense and target RNAs. (Upper panel) The 5′-most 90 nt of *lacI* mRNA. Regions complementary to segments of the antisense RNAs are indicated by brackets. The ribozyme cleavage site (black arrow) and the positions of putative RNase III cleavages (see Results and Fig. 7) are indicated (red arrows). The Shine–Dalgarno sequence and the GUG start codon of *lacI* are underlined. Solid dots are spaced by 10 nt for better orientation. (Lower panels) The left hand box shows, for comparison, the secondary structure of CopA RNA (22), from which the recognition units were derived. SL II represents the stem–loop segment encoded by pGW48 and contains the two *Sma*I sequences (mutational alterations in green). The two RNA stem–loops encoded by plasmids pGW48-a (a-SL II) and pGW48-s (s-SL II) are shown and sequences complementary (red) or corresponding to the targeted *lacI* sequence (blue) are indicated. The consensus secondary structure of a hairpin ribozyme (28) with its *lacI*-specific complementary flanking sequences (in red) is shown.

folding of the upper stem–loop, however, this region within s-SL II RNA is more exposed to single-strand-specific reagents, suggesting that the top three base pairs are not formed.

In vivo analysis of the plasmid-encoded antisense RNAs

The relative inhibitory efficiency of an antisense RNA depends on both its activity (e.g. binding/cleavage rate) and its intracellular concentration. Since it was conceivable that the stability of the various antisense RNAs could differ greatly, we performed an analysis of RNA extracted from strains that carried plasmids of the pGW48 series (as in Fig. 1). The use of Northern analysis permits quantification of relative RNA levels and permits an asessment of the intactness of the RNAs, i.e. provides information on specific decay intermediates and on aberrant termination. The probe used was directed against an RNA segment present in all RNAs and reprobing of the membrane for 5S rRNA permitted correction for loading.

The autoradiogram in Figure 4 (upper) and the summary of the relative signal intensities (lower) indicate that all antisense RNAs accumulate to similar intracellular concentrations. Stem–loop II of CopA (pGW47.1; Fig. 4) appears to be somewhat more stable than SLII containing the *Sma*I site sequences in the lower stem (pGW48, pGW48-a and pGW48-s; Fig. 4). All RNAs with insertions in front of SL II were ~2-fold more stable than the parental stem–loop RNA alone (encoded by pGW47-1).

The band pattern also shows that read-through of the SL II terminator occurs to an appreciable degree, ~7–9% in pGW48, pGW48-a and pGW48-s, as indicated by the appearence of bands consistent with termination at the plasmid-encoded fd terminator ~70 bp downstream of SL II (Fig. 4, open squares). This phenomenon is more pronounced when additional sequences are present in front of SL II (rib or rbs in either orientation; cf. Fig. 1B); signals of the ‘read-through’ bands are up to 2.5 times more intense than the bands of the correctly terminated ones (Fig. 4, open circles). Thus, either most transcripts fail to terminate at SL II, but terminate at the fd terminator, or the longer transcripts are more stable than the shorter ones. Since all RNAs are initiated at the same promoter, the latter possibility is more likely. In addition to the major bands, whose sizes are consistent with their expected lengths, we see a series of minor bands that most likely represent degradation intermediates. In conclusion, the Northern analysis shows that RNA sizes are as expected (taking into account a termination defect) and intracellular concentrations do not vary greatly in dependence on any of the sequences being present or absent.

Antisense RNA-mediated inhibition of LacI–LacZ fusion protein synthesis *in vivo*

In pilot experiments we transformed all cassette plasmids separately into an *E.coli* strain carrying a complete *lac* operon. Transformation and spreading on X-Gal indicator plates was expected to permit assessment of antisense activity by the appearance of blue colonies, since inactivation of *lacI* mRNA should derepress *lacZ* expression. The colonies obtained showed variations in blue colour intensity, but it proved difficult to use this test for quantification of effectiveness (data not shown).

Instead, plasmids were transformed into a bacterial strain that carried an F plasmid encoding a LacI–LacZ fusion protein (15). The fusion gene carries the wild-type *lacI* promoter and the 5′-portion of the *lacI* frame, as shown in Figure 2. LacI–LacZ fusion protein synthesis was measured in bacterial extracts and the data are presented in Table 2. Overall, inhibition by antisense RNAs was unexpectedly inefficient. The most efficient construct, pGW48-a-rbs, conferred an ~50% reduction in *lacI–lacZ* expression. Thus, the most efficient antisense RNA of the set tested carried both an anti-*lacI* recognition and an anti-RBS unit, i.e.

Downloaded from https://academic.oup.com/nar/article/25/16/3218/1454766 by guest on 10 April 2024

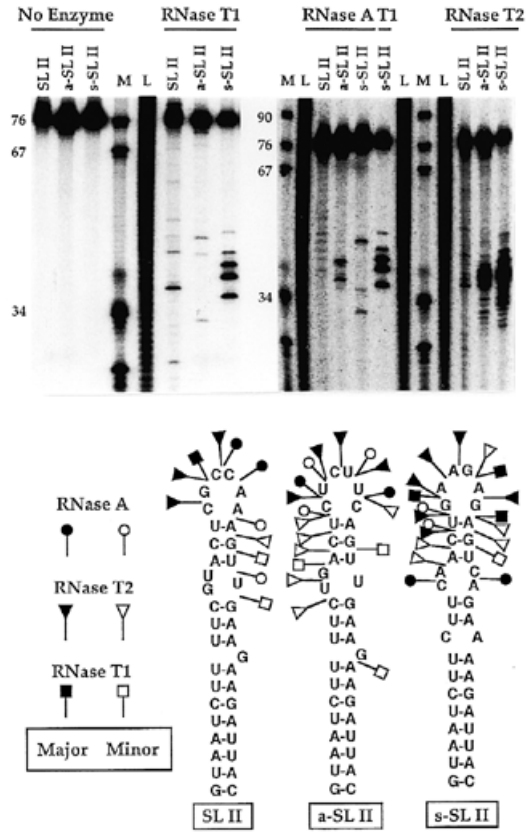

Figure 3. Secondary structure analysis of recognition unit RNA segments. Secondary structure probing was performed as in Materials and Methods. (Upper panel) An autoradiogram of partial digests performed on 5′-end-labelled RNAs. The sequencing gel was run to resolve the loop regions. SL II represents stem–loop II RNA of pGW48, a-SL II and s-SL II those of pGW48-a and pGW48-s respectively. RNases used are indicated above the lanes. M represents a molecular size marker (*Msp*I fragments of plasmid pBR322). Some relevant sizes are indicated. L is an alkaline ladder. The T1 digest of sense *lacI*–SL II in the right hand autoradiogram was included to facilitate assignment of cleavage products. (Lower panel) A graphic representation of cleavage sites obtained.

both in antisense orientation to *lacI* mRNA. Generally, all anti-*lacI* recognition units promoted weak, but significant, inhibition, whereas the sense units were inefficient. Contributions of ribozyme units were minor or negligible, whereas an anti-RBS unit in conjunction with a recognition unit in sense orientation inhibited to ~41%.

In vitro antisense/target RNA binding

The poor *in vivo* efficiency indicated in Table 2 could be a result of slow binding rates, in particular in the case of rbs units, and of ineffective cleavage in the case of ribozyme units. Complex formation between complementary (even partially complementary) RNAs can be conveniently studied using gel shift assays. An excess of unlabelled target RNA (Materials and Methods) was incubated with ^{32}P-labelled RNA, either a-rbs, s-rbs or, as controls, a-sbr and s-sbr RNA. Aliquots were withdrawn at different time points and complex formation measured (Fig. 5). Second order binding rate constants were calculated for the two rbs-containing RNA species (9). Both rbs RNAs, containing 38 nt complementary to the *lacI* RBS region, showed complex formation as a function of time, although the rate constants obtained (~3–6 × 10^4/M/s) were almost two orders of magnitude lower than those obtained with, for example, CopA/CopT (see for example 9). The contribution of the recognition stem–loop to binding rate was small: a recognition unit complementary to *lacI* (a-rbs, Fig. 5) was barely 2-fold more effective than the non-complementary one (s-rbs, Fig. 5). As expected, the sbr RNAs, which carry the 38 nt *lacI* segment in the sense orientation, did not form duplexes (Fig. 5).

Table 2. *lacI–lacZ* fusion gene expression in strains carrying antisense RNA gene cassettes

Plasmids[a]	Miller units[b]	Relative β-galactosidase activity[c]	Inhibition (%)
pMc5-8	111.7 ± 10.8	1.00	0
pGW47	98.6 ± 11.7	0.88	12
pGW47-1	93.2 ± 23.6	0.84	16
pGW48	88.6 ± 29.4	0.79	21
pGW48-a	61.6 ± 19.0	0.55	45
pGW48-s	99.3 ± 24.5	0.89	11
pGW48-a-rib	74.7 ± 8.8	0.67	33
pGW48-s-rib	83.9 ± 17.0	0.75	25
pGW48-a-bir	78.3 ± 8.0	0.70	30
pGW48-s-bir	95.5 ± 16.4	0.86	14
pGW48-a-rbs	56.2 ± 17.7	0.50	50
pGW48-s-rbs	66.2 ± 20.4	0.59	41
pGW48-a-sbr	70.1 ± 15.0	0.63	37
pGW48-s-sbr	106.3 ± 20.1	0.95	5

[a]Plasmids encoding antisense RNA gene cassettes present in strain XAc(F′[*lacI–lacZ* fusion]).
[b]Assays were performed as in Materials and Methods and represent averages of five independent determinations. The values obtained are represented in Miller units (18). Standard deviations are given.
[c]Miller units were converted to relative activities. The activity obtained with pMc5-8 was set to unity.

In vitro cleavage activity of ribozyme-containing RNAs

Since Table 2 indicated insignificant inhibitory activity of ribozyme-containing RNAs *in vivo*, we were concerned that the ribozyme-containing RNAs were inactive altogether. *In vitro* cleavage activity of a-rib and s-rib RNAs was assessed in a time course assay. Uniformly ^{32}P-labelled *lacI* RNA was cleaved and aliquots were separated on sequencing gels. The autoradiogram in Figure 6A shows that significant cleavage was obtained over 3 h and that the cleavage products were of the expected size. The antisense orientation of the *lacI* recognition stem–loop only enhanced the cleavage rate by a factor of two, compared with that in the sense orientation. Additional experiments were carried out with up to 100-fold different ribozyme concentrations. Since <3-fold increases in cleavage rate were measured, this indicates that the chemical step, rather than the binding step, is limiting the reaction rate. In order to map the exact location of the cleavage site, reactions were carried out using unlabelled RNAs, followed by reverse transcription. The resulting cDNA products were run on gels alongside sequencing ladders generated on *lacI* DNA using the same primer (Fig. 6B). The position of the cleavage

Downloaded from https://academic.oup.com/nar/article/25/16/3218/1454766 by guest on 10 April 2024

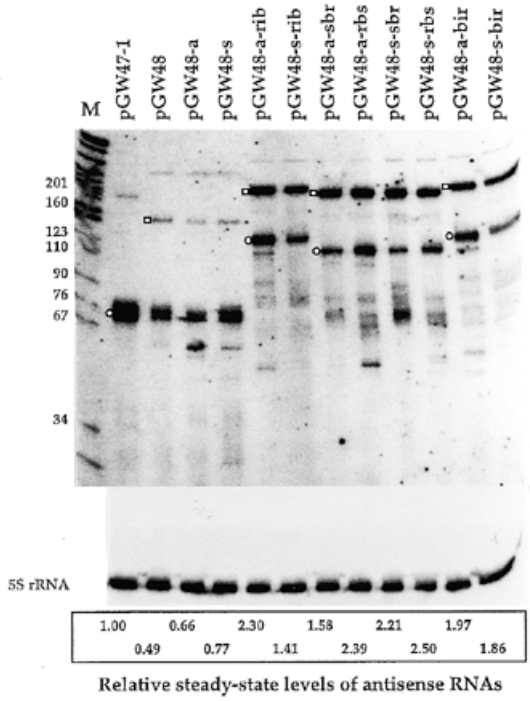

Figure 4. Northern analysis of *in vivo* RNAs encoded by cassette-carrying plasmids. Northern analysis was performed as described in Materials and Methods. The upper autoradiogram represents a membrane probed for all cassette-encoded RNAs and the lower autoradiogram a reprobing of the same membrane for 5S rRNA (loading control). Plasmids present in the strains are indicated. Approximate sizes are shown next to the autoradiogram. M is a size marker (*Msp*I fragments of pBR322 DNA). Circles indicate normally terminated RNAs, squares RNAs terminated at the fd terminator (see Results). Relative steady-state levels of antisense RNAs were calculated (sum of all band intensities corrected for loading) and are shown below.

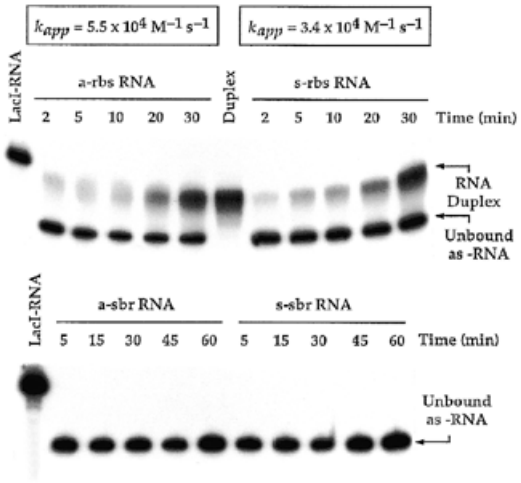

Figure 5. *In vitro* binding assay. Binding between ^{32}P-labelled antisense RNAs and a >10-fold excess of unlabelled *lacI* target RNA was performed as in Materials and Methods. The time points for sample withdrawal are indicated and positions for free and complexed antisense RNAs are shown. LacI-RNA indicates ^{32}P-labelled target RNA (149 nt) loaded for size comparison and Duplex indicates an artificially formed antisense/target RNA duplex (annealed by boiling and slow cooling). The boxes show the calculated pairing rate constants for the two rbs-containing RNA species.

(UAUCA⇓GACCG, the arrow indicates the cleavage site; see Fig. 2) was consistent with that expected from the design of the ribozyme sequence.

Primer extension analysis of target RNAs extracted from cells carrying antisense RNA-encoding plasmids

The rbs-containing RNAs are complementary to *lacI* mRNA over a region of 38 nt. If hybridization occurs *in vivo*, one can expect RNase III-dependent cleavage ~15 nt from the end of the helical region (see for example 24); this enzyme cleaves RNA duplexes of >2 helical turns (32). Primer extension analysis performed on RNA extracted from cells can therefore be used to compare signals representing the 5′-end of the target RNA to those generated by putative RNase III-dependent cleavage. 5′-Ends in the region of complementarity may indicate productive interaction *in vivo*. Similarly, if ribozyme-mediated cleavage occurred, this should be indicated by a cDNA product terminating at the site of cleavage. Figure 7 shows that no bands consistent with ribozyme-mediated cleavage of *lacI* mRNA are detectable, in line with the negligible inhibition shown in Table 2. This result does not permit us to conclude that cleavage *in vivo* does not occur, but indicates that a putative cleavage rate must be much slower than average degradation rates of resulting products. Band III may be a result of duplex-dependent RNase III cleavage of *lacI* mRNA, since it: (i) is generated only when cells carry rbs RNAs, with the complementary region indicated in Figure 2; (ii) the location of the deduced processing sites is located ~12 nt from the end of the predicted duplex region [site(s) shown in Fig. 2].

DISCUSSION

This communication describes a set of antisense RNA cassettes designed to silence chosen target genes, here exemplified by the *E.coli lacI* gene. The antisense RNA genes were built from cassettes (a promoter, an inhibitory unit and a recognition unit), all separated by suitable restriction sites. The rationale for this design was that an RNA element modelled according to recognition structures in naturally occurring antisense RNAs should promote rapid binding to a target sequence. Subsequently, an inhibitory segment of the RNA encoded by the gene cassette should bind to additional target sequences and promote inhibition of target RNA function. This could either be accomplished by sequestering of ribosome binding sites or by cleavage of the target RNA. In either case, inclusion of the recognition element was expected to render the base pairing rate of the inhibitory unit concentration independent. The antisense RNAs are thus non-contiguous in their complementarity to the target RNA and units can in principle be optimized separately.

The choice of the major CopA stem–loop II (SL II) as the parental recognition structure was based on previous studies: (i) stem–loops like SL II of CopA (10,11), stem–loops of RNA I (ColE1; 33) and that of RNA-OUT (Tn*10*; 34) are implicated in the rate determining step of target RNA binding; (ii) the rate of CopA/CopT binding is essentially diffusion controlled and therefore at a maximum (11,12); (iii) the structure of CopA is crucial for rapid target RNA binding, Hjalt and Wagner (20,31) having shown that changes in loop size as well as removal of characteristic bulged out nucleotides have detrimental effects on binding rate *in vitro* and inhibition *in vivo*; (iv) a growing body of evidence indicates that antisense/target RNA complexes can be inhibitory without

Downloaded from https://academic.oup.com/nar/article/25/16/3218/1454766 by guest on 10 April 2024

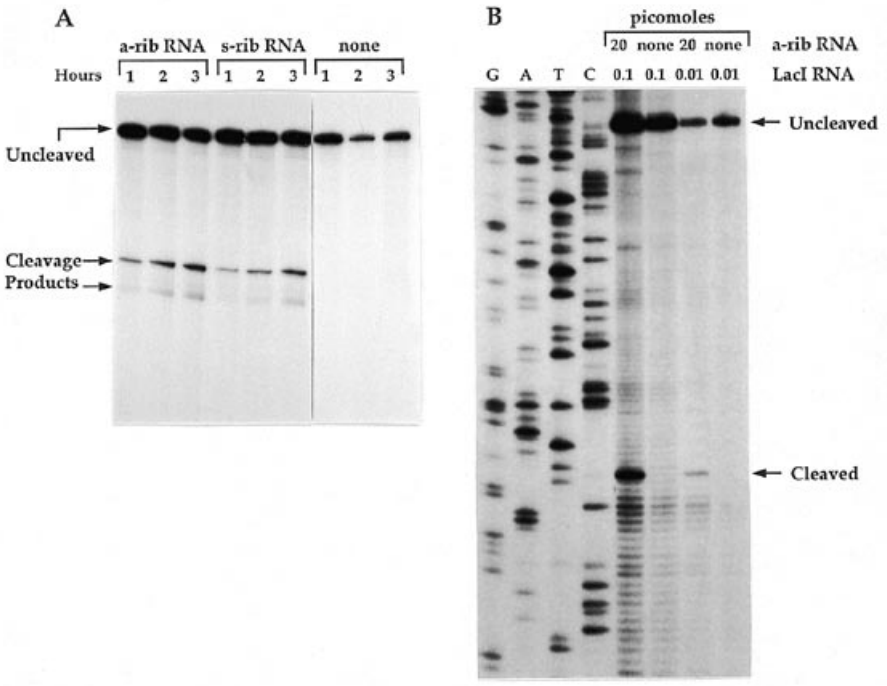

Figure 6. *In vitro* cleavage activity of ribozyme-containing RNAs and determination of the cleavage site. (**A**) Cleavage assays were performed using uniformly ^{32}P-labelled *lacI* RNA and a molar excess of unlabelled ribozyme-containing RNAs (a-rib and s-rib). Aliquots were withdrawn at the times indicated and fragments resolved on a sequencing gel. (**B**) Identification of the cleavage site was by primer extension analysis (see Materials and Methods) of parallel samples (both RNAs unlabelled). The positions of the 5′-end of *lacI* RNA (Uncleaved) and the 5′-end generated by cleavage (Cleaved) are indicated. The sequencing ladder was generated by dideoxy sequencing of *lacI* DNA using the reverse transcription primer.

forming complete duplexes (see 35,36 and references therein). Thus, we inferred that a recognition stem–loop that promotes fast binding should resemble, as closely as possible, CopA SL II. Hence, care was taken to construct SL II elements that both carried sequence complementarity to *lacI* RNA in the upper stem–loop region and preserved the CopA-like structure. Secondary structure probing using structure-specific ribonucleases (Fig. 3) and Pb(II) acetate (data not shown) confirmed that antisense *lacI* SL II carried a stem–loop structure close to the parental one. Determinations of steady-state levels of the antisense RNAs in cells carrying the cassette-containing plasmids indicated ~2- to 3-fold variations in concentration, indicating that fairly great variations in sequence and (presumed) secondary structure can be tolerated without major effects on antisense RNA half-life (Fig. 4). This figure also indicates that the presence of ribozyme or anti-RBS RNA sequences, in either orientation, markedly affected termination at SL II.

When the series of antisense RNAs was tested for inhibiton of LacI–LacZ fusion protein synthesis, relatively small effects were observed (Table 2). Generally, antisense RNAs carrying SL II sequences complementary to the 5′-segment of *lacI* mRNA (all pGW48-a variants) showed low but significant inhibition, whether or not they were combined with inhibitory units. Similarly, the presence of sequences complementary to the *lacI* RBS showed inhibition, whereas the sense orientation was ineffective, as was the ribozyme sequence in either orientation. The strongest inhibition obtained, 50%, was obtained with the RNA encoded by pGW48-a-rbs, i.e. with both the recognition loop and RBS unit in antisense orientation. It is conceivable that the contribution of the anti-*lacI* stem–loop *alone* to inhibition may be underestimated, since this RNA (pGW48-a; Fig. 4) is ~3-fold less abundant in steady-state than either of the rbs/sbr/bir/rib-containing RNAs.

In vitro binding of rbs RNAs to target RNA was measured (Fig. 5) and shown to occur at a rate ~100-fold slower than that obtained with natural antisense/target RNA combinations (see for example 9). The rate enhancement conferred by SL II was surprisingly small (2-fold in antisense orientation; Fig. 5). Low rates in the 10^4/M/s range are indicative of RNAs whose structures are not optimized for binding. For instance, *in vitro* binding of two complementary RNAs derived from the coding region of the *repA* gene of plasmid R1 yielded similar values (Söderbom and Wagner, unpublished) and, in a study of artificial anti-HIV RNAs, Homann *et al.* (7) measured association rate constants ranging from 0.3 to 4.0×10^4/M/s. Since *in vitro* binding of the rbs RNAs was slow, it appears likely that the inefficiency of inhibition (Table 2) is mainly due to slow rates of duplex formation *in vivo*. Congruent with this, most of the target RNA is intact, as judged from a primer extension analysis (Fig. 7). Only a minor fraction of *lacI* mRNA appears to be cleaved within the region of complementarity (see Fig. 2 for cleavage site). This cleavage, which occurs only in cells carrying rbs-containing antisense RNAs, is most likely catalysed by RNase III, as demonstrated in a variety of systems (see for example 24,37). In line with the superior inhibitory activity of a-rbs over s-rbs (Table 2), the ratio of the band denoted III over the band corresponding to the 5′-end of *lacI* mRNA was increased.

It is intriguing that natural antisense RNAs are rapid binders with association rate constants in the 10^6/M/s range, whereas

Downloaded from https://academic.oup.com/nar/article/25/16/3218/1454766 by guest on 10 April 2024

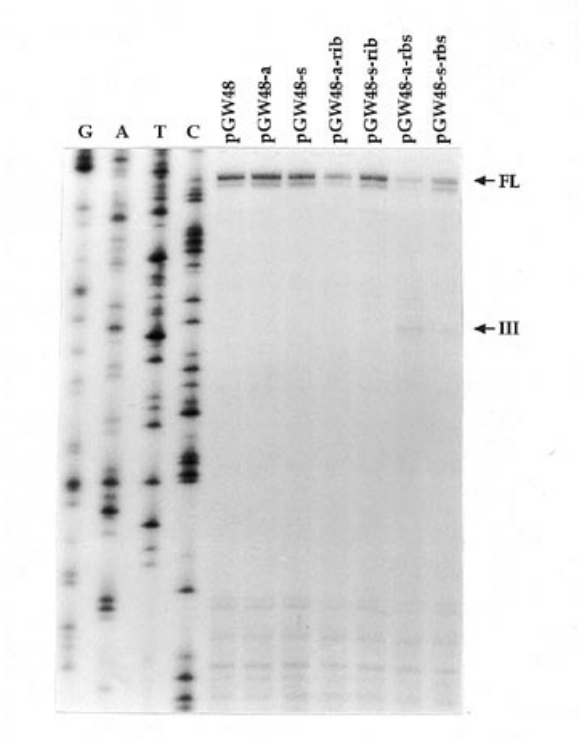

Figure 7. Mapping of *in vivo* 5′-ends of target RNAs. Total RNA was extracted from cells carrying antisense and target RNA genes and subjected to primer extension analysis as in Materials and Methods. Plasmids carrying the antisense RNA cassettes are indicated. Arrows show the 5′-ends of the transcription start site of *lacI* mRNA (FL) and 5′-ends generated by rbs RNA-dependent processing (III; see Results). The position of III is additionally indicated in Figure 2. GATC represent dideoxy sequencing ladders generated on *lacI* DNA using the reverse transcription primer.

most artificially created antisense RNAs are ~100-fold less effective (see above). Rapid association is crucial for the function of replication inhibitors in plasmids. It is therefore not surprising that the stem–loop recognition motifs commonly found in plasmid-encoded antisense RNAs (8) may have arisen under selective pressure for fast interaction. Nevertheless, as our data indicate, we still have too little insight into the factors that determine this property and, hence, cannot yet tailor such structures to any chosen target sequence.

In contrast to the limited, yet significant, inhibition by rbs RNA, all units containing hairpin ribozymes were ineffective (Table 2). *In vitro* ribozyme activity assays indicated that cleavage rates were very low and that the presence of a cognate recognition stem–loop only accelerated the reaction by a factor of two. Figure 6A indicates that, under the conditions used, >3 h are required to cleave half of the target RNA molecules. Since higher ribozyme concentrations only moderately enhanced the rate of cleavage, we infer that the chemical step rather than the association step is limiting. In agreement with this inefficient catalytic activity, we failed to observe cleavage of target RNA *in vivo* (Fig. 7) at the site mapped *in vitro* (Fig. 6B).

From the data presented, it is clear that the degree of inhibition obtained is unsatisfactory. For most gene silencing applications >>10-fold inhibition is desirable. The results reported here indicate some of the difficulties encountered and may point out what is required to improve performance. Since target RNA binding is a function of both the concentration of the antisense RNA and the binding rate constant, an increase in either one or both of these factors should improve inhibition. Daugherty *et al*. (5) obtained strong inhibition of *lacZ* expression with antisense RNAs directed against a large 5′-segment of the target RNA when the antisense/target RNA ratio was >100. Intracellular concentrations were not estimated, so that a direct comparison with the results presented here is not possible. From the Northern analysis in Figure 4 we estimate that antisense RNA concentrations ranged from 0.1 to 1 μM, which in the case of an efficient natural antisense RNA results in >95% inhibition (12). If the specific inhibitory efficiency of an artificial antisense RNAs is low, a great increase in steady-state level can compensate for this deficiency. Protective 5′ stem–loops could be used to protect RNAs from 5′-initiated degradation (38), to increase metabolic stability and intracellular concentration. Selection of rapidly binding RNAs from a pool of complementary species differing in their extent of complementarity (39) may be used to enhance binding substantially. Since the half-life of typical bacterial mRNAs is in the range 2–4 min (40), it is likely that binding rate constants in the 10^4/M/s range are insufficient to inactivate a substantial fraction of the target RNAs.

The experiments shown in Figure 6 and Table 2 indicate that catalytic RNAs may not be suitable as efficient inhibitors in bacterial systems. Even a considerably increased cleavage rate would only marginally improve inhibition (mRNA half-lives of 2–4 min compared with cleavage rates of more than a generation time), in particular since an increased intracellular concentration would not result in a corresponding increase in target cleavage (see above). A report of hammerhead ribozyme-dependent inhibition of proliferation of RNA coliphage SP in *E.coli* is pertinent to the same limitation of this approach (41), but a different, recent study indicates that >90% inhibition can be obtained (target *lacZ*; 42). It is likely that the differences in target RNA half-lives between prokaryotes and eukaryotes are responsible for the greater success of ribozyme strategies in the latter type of organism (43,44).

Analysis of the performance of the two unit antisense RNAs described here indicates what modifications may be beneficial for improved inhibitory potential. Since the cassettes are separated by suitable restriction sites, separate optimization protocols can be used. The choice of stronger, inducible promoters is expected to yield some increase in inhibition. Randomized sequences introduced in the region encoding the upper portion of the recognition stem–loop (bordered by *Sma*I/*Xma*I sites) can be used to select rapid binders of *in vitro* synthesized target RNA. The small, but significant, effect of the recognition unit alone (Table 2) suggests that RNAs consisting of multiple stem–loop units each with its own separate target complementarity may be effective. Inhibition units can be kinetically selected from complementary sets of anti-RBS sequences as in Rittner *et al*. (39). In addition, the introduction of RNA stability elements at the 5′- and/or 3′-ends of the antisense RNA should permit accumulation of higher concentrations of the inhibitor. Even the combination of only moderately improved units should thus yield a substantial increase in antisense RNA efficiency. Finally, it is conceivable that the choice of the target RNA may affect the degree of inhibition that can be obtained. We have therefore begun to adopt a similar strategy using plasmid-encoded *bla* mRNA as an inhibition model.

In conclusion, we suggest that the pitfalls of antisense RNA design require thorough study of the parameters crucial for inhibition. We believe that the approach taken here may be helpful to obtain versatile and easily optimizable antisense RNA inhibitors.

Downloaded from https://academic.oup.com/nar/article/25/16/3218/1454766 by guest on 10 April 2024

ACKNOWLEDGEMENT

This work was supported by a grant from the Swedish Board of Engineering Sciences (TFR) to E.G.H.Wagner.

REFERENCES

1 Nellen,W. and Lichtenstein,C. (1993) *Trends Biochem. Sci*., **18**, 419–423.
2 Matteucci,M.D. and Wagner,R.W. (1996) *Nature*, **384** (suppl.), 20–22.
3 Wagner,R.W. (1994) *Nature*, **372**, 333–335.
4 Milligan,J.F., Matteucci,M.D. and Martin,J.C. (1993) *J. Med. Chem*., **36**, 1923–1937.
5 Daugherty,B.L., Hotta,K., Kumar,C., Ahn,Y.H., Zhu,J. and Pestka,S. (1989) *Gene Anal. Techniques*, **6**, 1–16.
6 Gray,J., Picton,S., Shabbeer,J., Schuch,W. and Grierson,D. (1992) *Plant Mol. Biol*., **19**, 69–87.
7 Homann,M., Rittner,K. and Sczakiel,G. (1993) *J. Mol. Biol*., **233**, 7–15.
8 Wagner,E.G.H. and Simons,R.W. (1994) *Annu. Rev. Microbiol*., **48**, 713–742.
9 Persson,C., Wagner,E.G.H. and Nordström,K. (1988) *EMBO J*., **7**, 3279–3288.
10 Persson,C., Wagner,E.G.H. and Nordström,K. (1990) *EMBO J*., **9**, 3767–3776.
11 Persson,C., Wagner,E.G.H. and Nordström,K. (1990) *EMBO J*., **9**, 3777–3785.
12 Nordström,K. and Wagner,E.G.H. (1994) *Trends Biochem. Sci*., **19**, 294–300.
13 Farabaugh,P.J. (1978) *Nature*, **274**, 765–769.
14 Hanahan,D. (1985) In Glover,D.M. (ed.), *DNA Cloning I*. IRL Press, Oxford, UK, pp. 109–135.
15 Miller,J.H., Coulondre,C. and Farabaugh,P.J. (1978) *Nature*, **274**, 770–775.
16 Stanssens,P., Opsomer,C., McKeown,Y.M., Kramer,W., Zabeau,M. and Fritz,H.J. (1989) *Nucleic Acids Res*., **17**, 4441–4454.
17 Bertani,G. (1951) *J. Bacteriol*., **62**, 293–300.
18 Miller,J.H. (1972) *Experiments in Molecular Genetics*. Cold Spring Harbor Laboratory Press. Cold Spring Harbor, NY, pp. 352–355.
19 Sambrook,J., Fritsch,E.F. and Maniatis,T. (1989) *Molecular Cloning: A Laboratory Manual*. Cold Spring Harbor Laboratory Press. Cold Spring Harbor, NY.
20 Hjalt,T.H. and Wagner,E.G.H. (1992) *Nucleic Acids Res*., **20**, 6723–6732.
21 Dretzen,G., Bellard,M., Sassone-Corsi,P. and Chambon,P. (1981) *Anal. Biochem*., **112**, 295–298.
22 Wagner,E.G.H. and Nordström,K. (1986) *Nucleic Acids Res*., **14**, 2523–2538.
23 Hjalt,T.Å.H. and Wagner,E.G.H. (1995a) *Nucleic Acids Res*., **23**, 571–579.
24 Blomberg,P., Wagner,E.G.H. and Nordström,K. (1990) *EMBO J*., **9**, 2331–2340.
25 Chowrira,B.M. and Burke,J.M. (1991) *Biochemistry*, **30**, 8518–8522.
26 Berzal-Herránz,A., Wagner,E.G.H. and Diaz-Orejás,R. (1991) *Mol. Microbiol*., **5**, 97–108.
27 Berzal-Herránz,A., Joseph,S. and Burke,J. (1992) *Genes Dev*., **6**, 129–134.
28 Berzal-Herránz,A., Joseph,S., Chowrira,B.M., Butcher,S.E. and Burke,J.M. (1993). *EMBO J*., **12**, 2567–2574.
29 Chowrira,B.M., Berzal-Herranz,A. and Burke,J.M. (1991) *Nature*, **354**, 320–322.
30 Chowrira,B.M., Berzal-Herranz,A. and Burke,J.M. (1993) *Biochemistry*, **32**, 1088–1095.
31 Hjalt,T.Å.H. and Wagner,E.G.H. (1995b) *Nucleic Acids Res*., **23**, 580–587.
32 Court,D. (1993) In Belasco,J.G. and Brawerman,G. (eds), *Control of Messenger RNA Stability*. Academic Press, San Diego, CA, pp. 71–116.
33 Tomizawa,J. (1984) *Cell*, **38**, 861–870.
34 Kittle,J.D., Simons,R.W., Lee,J. and Kleckner,N. (1989) *J. Mol. Biol*., **210**, 561–572.
35 Wagner,E.G.H., Blomberg,P. and Nordström,K. (1992) *EMBO J*., **11**, 1195–1203.
36 Malmgren,C., Wagner,E.G.H., Ehresmann,C., Ehresmann,B. and Romby,P. (1997) *J. Biol. Chem*., **272**, 12508–12512.
37 Case,C.C., Simons,E.L. and Simons,R.W. (1990) *EMBO J*., **9**, 1259–1266.
38 Bouvet,P. and Belasco,J.G. (1992) *Nature*, **360**, 488–491.
39 Rittner,K., Burmester,C. and Sczakiel,G. (1993) *Nucleic Acids Res*., **21**, 1381–1387.
40 Belasco,J. (1993) In Belasco,J.G. and Brawerman,G. (eds), *Control of Messenger RNA Stability*. Academic Press, San Diego, CA, pp. 3–12.
41 Inokuchi,Y., Yuyama,N., Hirashima,A., Nishikawa,S., Ohkawa,J. and Taira,K. (1994) *J. Biol. Chem*., **269**, 11361–11366.
42 Junn,E. and Kang,C. (1996) *Genet. Anal*., **13**, 1–7.
43 Altman,S. (1993) *Proc. Natl. Acad. Sci. USA*, **90**, 10898–10900.
44 Couture,L.A. and Stinchcomb,D.T. (1996) *Trends Genet*., **12**, 510–515.

Downloaded from https://academic.oup.com/nar/article/25/16/3218/1454766 by guest on 10 April 2024